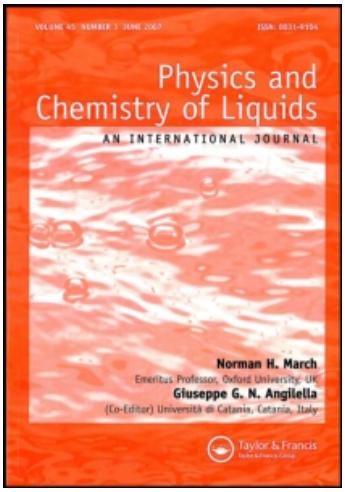

Physics and Chemistry of Liquids
Publication details, including instructions for authors and subscription information:
http://www.informaworld.com/smpp/title~content=t713646857

New equation of state for double Yukawa potential with application to Lennard-Jones fluids

M. Bahaa Khedr[a]; S. M. Osman[b]; M.S. Al Busaidi[b]
[a] Faculty of Science, Physics Department, Banha University, Banha, Egypt [b] Physics Department, Sultan Qaboos University, Muscat, Oman

To cite this Article Bahaa Khedr, M. , Osman, S. M. and Busaidi, M.S. Al(2009) 'New equation of state for double Yukawa potential with application to Lennard-Jones fluids', Physics and Chemistry of Liquids, 47: 3, 237 — 249
To link to this Article: DOI: 10.1080/00319100802428494
URL: http://dx.doi.org/10.1080/00319100802428494

Physics and Chemistry of Liquids
Vol. 47, No. 3, June 2009, 237–249

Taylor & Francis
Taylor & Francis Group

New equation of state for double Yukawa potential with application to Lennard–Jones fluids

M. Bahaa Khedr[a], S.M. Osman[b]* and M.S. Al Busaidi[b]

[a]*Faculty of Science, Physics Department, Banha University, Banha, Egypt;* [b]*Physics Department, Sultan Qaboos University, Muscat, Oman*

(*Received 31 May 2008; final version received 23 August 2008*)

We present a simple but accurate equation of state for double Yukawa fluids based on the variational series mean spherical approximation (VSMSA). This allows us to investigate the vapour–liquid equilibrium and its related thermodynamic properties. The comparisons with computer simulation results of the Lennard–Jones (LJ) potential suggest the importance of treating the attractive tail of the potential accurately via VSMSA. The estimated reduced critical parameters $T_C = 1.342$, $\rho_C = 0.29$ and $P_C = 0.135$ are in good agreement with other theoretical and computer simulation results for the LJ system.

Keywords: theory of simple liquids; equation of state of simple liquids; properties of double Yukawa potential; liquid–vapour coexistence

1. Introduction

Phase equilibrium properties of fluids form the basis for large numbers of separation techniques used by process industries, and are used to investigate the behaviour of a wide class of physical systems. The goal of research in this area is to develop a fundamentally sound methodology for the calculation of the physical properties of coexisting phases at equilibrium [1,2]. The prediction of phase equilibrium from the knowledge of the interatomic forces of classical systems can now be done quite accurately. This is mainly due to considerable progress in advanced perturbation theories [3–8], variational theories [1,9,10] and computer simulation methods [11–20] which has taken place over the last 30 years. In general, these perturbation techniques introduce a number of errors. To minimise such errors, one has to use an adequate and accurate reference system formalism and adopt a suitable criteria for calculating the effective hard-sphere (HS) diameter, σ, at each temperature, T, and density, ρ.

Recently, Henderson *et al*. [21] and Duh and Mier-y-Teran [22] reported an explicit non-empirical equation of state (EOS) for hard-sphere plus single Yukawa (HSY) potential based on the inverse temperature expansion of the pair correlation function at contact, within the exact solution of the mean spherical approximation (MSA), which is known as series mean spherical approximation (SMSA). The SMSA reproduced very accurate thermodynamic properties for HSY fluids, comparable to Gibbs ensemble Monte Carlo (GEMC) computer simulation results, except in the vicinity of the vapour–liquid

*Corresponding author. Email: osm@squ.edu.om

ISSN 0031–9104 print/ISSN 1029–0451 online

DOI: 10.1080/00319100802428494
http://www.informaworld.com

critical point [22]. In the present work, we adopt the SMSA for double Yukawa (DY) fluid and apply the Gibbs–Bogoliubov (GB) variational theory [9,10] for the accurate determination of the HS diameter. The resulting EOS is called variational series mean spherical approximation (VSMSA).

Several authors [23–28] have shown that the DY potential, with suitably chosen parameters, provides accurate thermodynamic properties for simple liquids. The function form of DY potential with four fitting parameters σ_0, E, λ_1 and λ_2 reads,

$$\varphi_{\mathrm{DY}}(r^*) = \frac{E\varepsilon_0}{r^*}\left[e^{-\lambda_1(r^*-1)} - e^{-\lambda_2(r^*-1)}\right]. \tag{1}$$

The more realistic continuous potential for spherically symmetric, non-polar real fluids is the Lennard–Jones (LJ) model potential, $\varphi_{\mathrm{LJ}}(r^*)$,

$$\varphi_{\mathrm{LJ}}(r^*) = 4\varepsilon_0\left[r^{*^{-12}} - r^{*^{-6}}\right]. \tag{2}$$

In Equations (1) and (2), $r^* = r/\sigma_0$ is the reduced intermolecular separation, and σ_0 and ε_0 are known to be the position of the zero potential and the depth of the attractive well, respectively. The LJ potential is chosen because it is the best studied continuous potential so far ([29] and the references therein) and it gives a reasonable approximate representation of the properties of real fluids. The LJ potential has the disadvantage of not being analytically solvable in any integral equation approximation valid in dense fluid regions. On the other hand, the DY potential has two major advantages: first, it can closely mimic any realistic or empirical potential, even those with extremely soft core or short-ranged attractive tail; second, the DY exponential form renders the MSA analytical solution [30]. Moreover, it facilitates the use of the Laplace transform of the HS radial distribution function ($rg_{\mathrm{HS}}(r)$), hence it leads to analytical EOS [24–27]. Thus the DY potential, Equation (1), is an intrinsically interesting simple potential that can be used in testing theoretical approaches to simple fluids. For the above-mentioned reasons, we performed a least-square fit to the LJ potential with the DY potential by fixing the zero position and minimum position via the parameters σ_0 and ε_0, and varying the adjustable parameters E, λ_1 and λ_2. The best fit parameters are

$$E = 2.0198, \quad \lambda_1 = 14.7350, \quad \lambda_2 = 2.6793. \tag{3}$$

The two potentials functions are presented in Figure 1. The aim of this work is to introduce a new method for calculating the thermodynamic properties along the vapour–liquid equilibrium (VLE) curve for LJ fluids, for which we propose DY potential model with parameters given in Equation (3). The link between the HS reference system and the perturbation part of the potential is established via the GB method [9,10]. We find it more convenient, before proceeding further, to introduce the following reduced quantities for future reference. For the effective HS diameter $\sigma^* = \sigma/\sigma_0$, the density $\rho^* = \rho\sigma_0^3$, temperature $T^* = (\beta\varepsilon_0)^{-1}$, pressure $P^* = P\sigma_0^3/\varepsilon_0$, isothermal compressibility $\chi_T^* = \chi_T(\varepsilon_0/\sigma_0^3)$, internal energy $U^* = U/N\varepsilon_0$ and the chemical potential $\mu^* = \mu/N\varepsilon_0$ with $\beta = (k_{\mathrm{B}}T)^{-1}$, where k_{B} is the Boltzman's constant. The layout of our article is as follows: in Section 2, we present the EOS for DY fluids based on the VSMSA. In Section 3, we assess the accuracy of the proposed EOS by extensive comparison with earlier theoretical results and computer simulation results for LJ fluids, followed with brief concluding remarks in Section 4.

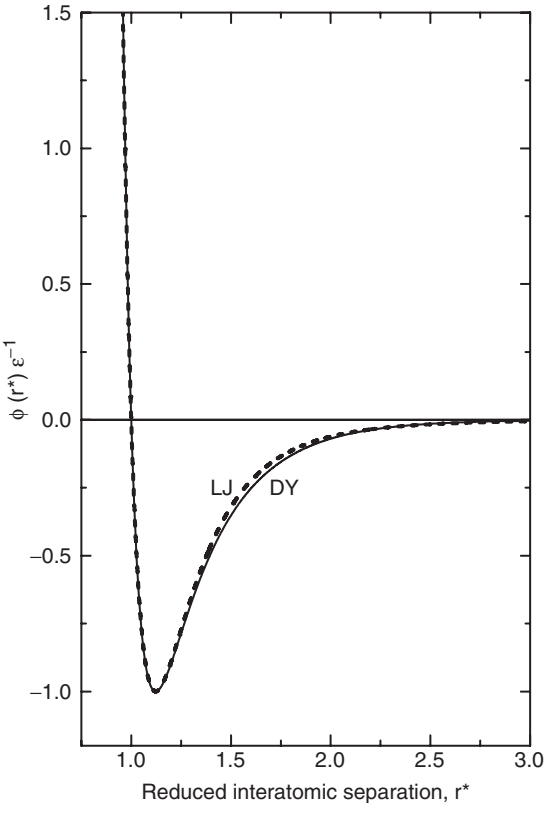

Figure 1. Intermolecular potential of LJ fluid. The usual LJ potential (dashed line) and the fitted DY potential (solid line).

2. Equation of state

Both perturbation theory and variational theory of fluids depend on the decomposition of a specified pair potential $\varphi(r)$ into reference part $\varphi_0(r)$ and weak perturbation part $\varphi_t(r)$, such that

$$\varphi(r) = \varphi_0(r) + \varphi_t(r). \tag{4}$$

Usually, $\varphi_0(r)$ is replaced by the familiar HS potential, characterised with effective HS diameter σ, which could be considered as a temperature and density dependent parameter. Here we replace $\varphi_t(r)$ by $\varphi_{\mathrm{DY}}(r^*)$, in Equation (1), but for $r > \sigma$. Accordingly, the Helmholtz free energy per particles of the system is a function of number density, ρ, and temperature, T, and can be written within the variational theory of classical fluid [9,10] as

$$\beta F = \beta F_{\mathrm{HS}} + \beta F_t, \tag{5}$$

where F_{HS} is the free energy of reference system; normally the system as HSs and F_t corresponds to the contribution from $\varphi_t(r)$. As regards to the choice of the reference system, we chose a suitable combination of the ideal gas contribution, F_{id}, and the scaled particle theory formalism for HS entropy due to Baus and Colot (BC) [31], $F_{\mathrm{ex}}^{\mathrm{BC}}$, namely

$$\beta F_{\mathrm{HS}} = \beta F_{\mathrm{id}} + \beta F_{\mathrm{ex}}^{\mathrm{BC}}, \tag{6}$$

$$\beta F_{\mathrm{id}} = -1 + \ln(\rho) - \frac{3}{2}\ln(T) - \frac{3}{2}\ln\left[\frac{2\pi m k_{\mathrm{B}}}{h^2}\right], \tag{7}$$

$$\beta F_{\mathrm{ex}}^{\mathrm{BC}} = (a + 3b - 1)\ \ln(1-\eta) + \frac{(6 + 2a + 6b)\eta - (3 + 3a + 9b)\eta^2 + 2b\eta^3}{2(1-\eta)^2}. \tag{8}$$

The last term in Equation (7) has no effect in calculating the VLE curve; however, m denotes the molecular mass and h is the Planck's constant. In Equation (8), $a = b = 2/3$ and $\eta = ((\pi/6)\rho\sigma^3)$ is the packing fraction. The first-order perturbation contribution reads

$$\beta F_t = 2\pi\rho \int_{\sigma}^{\infty} \beta\varphi_{\mathrm{DY}}(r) g_{\mathrm{HS}}(r) r^2\, \mathrm{d}r, \tag{9}$$

where $g_{\mathrm{HS}}(r)$ is the HS radial distribution function. The use of the DY potential further facilitates the acquisition of an analytic expression for F_t by introducing the Laplace transform of $(rg_{\mathrm{HS}}(r))$, defined as

$$G(\lambda) = \int_0^{\infty} r g_{\mathrm{HS}}(r)\, e^{-\lambda r}\, \mathrm{d}r. \tag{10}$$

Equations (1), (9) and (10) yield

$$\beta F_t = \frac{12\eta E}{\sigma^* T^*}\left[e^{\lambda_1}\ G(\lambda_1^*) - e^{\lambda_2}\ G(\lambda_2^*)\right]. \tag{11}$$

Here, $\lambda^* = \lambda\sigma^*$. One can readily derive analytic expressions for the pressure, P, and the chemical potential, μ, from Equation (5), via the standard thermodynamic relations $\beta P = \rho^2(\partial\beta F/\partial\rho)_T$ and $\beta\mu = \beta F + (\beta P/\rho)$, as the sum of HS and perturbation contributions

$$\beta P = \beta P_{\mathrm{HS}} + \beta P_t \tag{12}$$

and

$$\beta\mu = \beta\mu_{\mathrm{HS}} + \beta\mu_t. \tag{13}$$

It is straightforward to carry out the derivative, with respect to ρ, for F_{id}, F_{HS} and F_t of Equations (7), (8) and (11), respectively, yielding

$$\beta P_{\mathrm{HS}}^{\mathrm{BC}} = \frac{1 + \eta + \eta^2 - a\eta^3 - b\eta^4}{(1-\eta)^3}, \tag{14}$$

$$\frac{\beta P_t}{\rho} = \beta F_t + \frac{12E\eta^2}{\sigma^* T^*}\left[e^{\lambda_1} G'(\lambda_1^*) - e^{\lambda_2}\ G'(\lambda_2^*)\right], \tag{15}$$

where $G'(\lambda^*) = (\partial G(\lambda^*)/\partial\eta)_T$. Then the chemical potential contributions are simply

$$\beta\mu_{\mathrm{HS}} = \beta F_{\mathrm{HS}} + \frac{\beta P_{\mathrm{HS}}}{\rho} \quad \text{and} \quad \beta\mu_t = \beta F_t + \frac{\beta P_t}{\rho}. \tag{16}$$

The detailed expression of $G(\lambda^*)$ can be obtained in an analytical form from the recently developed SMSA of [21,22]:

$$G(\lambda) = \frac{e^{-\lambda^*}}{24\eta} \sum_{n=1}^{5} \frac{V_n(\lambda^*, \eta)}{n(T^*)^{n-1}}. \tag{17}$$

The sub-functions $V_n(\lambda^*, \eta)$ are given in closed analytical form in [22]. We carried out the derivatives, $V_n'(\lambda^*, \eta)$, analytically, with respect to η, but the final expression is quite lengthy to communicate in the present article.

The temperature and density dependence of the effective HS diameter σ can be introduced via the GB variational approach [9,10], $\beta F \leq \beta F_{\mathrm{HS}} + \beta F_t$, namely,

$$\left(\frac{\partial \beta F}{\partial \sigma}\right)_{\rho, T} = 0 \quad \text{at } \sigma_{\mathrm{GB}}. \tag{18}$$

It may be noted that the optimising diameter σ achieves a best free energy estimate of Equation (5) and establishes the link between F_{HS} and F_t.

The scaled particle theory (SPT) formalism, Equations (8) and (14), for HS fluid lead to three well-known equations of state according to the scaling parameters a and b. For example, $a = b = 0$ (compressibility EOS), $a = 3$, $b = 0$ (virial EOS) and $a = 1$, $b = 0$ (Carnahan–Starling EOS). BC [31] suggested the values $a = b = 2/3$. The comparison of the performance of the four equations of state with both MC and MD computer simulations results of the compressibility factor $Z_{\mathrm{HS}} = (P_{\mathrm{HS}}/\rho k_{\mathrm{B}} T)$ suggested the superiority of the SPT equation of state based on the BC estimated parameters ($a = b = 2/3$) on the other theoretical equations of state.

3. Results and discussion

We begin with the evaluation of the free energy and pressure contributing terms in order to visualise the effect of each component on the EOS. Typical results are shown in Table 1 for the entire density range at each temperature, covering the temperature range of the vapour–liquid phase diagram of LJ fluid. In principle, the free energy and pressure are quite sensitive to density variations. At low densities, the main effect comes from the HS contribution; by increasing density the attractive tail contribution builds up considerably. The same trend is observed at all temperatures. Moreover, we present the value of each term in the summation of the SMSA, given by Equations (11), (15) and (17). Important features of the series expansion are found. The main contribution is always due to the first term while the higher order terms show dramatic decrease in magnitude. The third and fourth terms contribute only at intermediate densities, while the fifth term has almost negligible effect at all densities.

To assess the performance of the present EOS, we present extensive comparison in Tables 2–5 with reported theoretical results from other equations of state and with the computer simulation results available for LJ fluid. In Tables 2 and 3, we present our estimate of the free energy and pressure, respectively, which are compared with a similar EOS reported by Gonzalez and Silbert [24] and with results of the pioneering Monte Carlo simulations of Hansen [32]. Gonzalez and Silbert [24] reported an EOS of DY potential fitted to LJ potential but with the variational Percus-Yevike approximation (VPY), i.e. the GB method was also used and the Laplace transform of PY radial distribution function

Table 1. The Helmholtz free energy components and pressure components as in the present EOS together with the respective components of F_t and P_t due to series expansion terms (for comparison).

		Helmholz free energy $\frac{F}{N\varepsilon_0}$							
T*	**ρ***	**F**	F_{hs}^{BC}	$\mathbf{F_t}$	$\mathbf{F_{t1}}$	$\mathbf{F_{t2}}$	$\mathbf{F_{t3}}$	$\mathbf{F_{t4}}$	$\mathbf{F_{t5}}$
		Eq. (5)	Eq. (6)	Eq. (11)	**Series terms** Eqs. (11) and (17)				
0.7	0.01	−3.60857	−3.53702	−0.07156	−0.05884	−0.01241	−0.00029	−0.00001	0.00000
	0.1	−2.51284	−1.80903	−0.70380	−0.60322	−0.07817	−0.01812	−0.00348	−0.00081
	0.5	−3.21411	0.08714	−3.30125	−3.29691	0.04322	−0.02952	−0.01229	−0.00575
	0.9	−3.69524	2.12077	−5.81602	−5.92336	0.10716	0.00063	−0.00034	−0.00010
1.0	0.01	−5.65535	−5.58811	−0.06724	−0.05855	−0.00853	−0.00015	0.00000	0.00000
	0.1	−3.78552	−3.12151	−0.66401	−0.60017	−0.05345	−0.00899	−0.00121	−0.00020
	0.5	−3.68312	−0.44284	−3.24028	−3.25688	0.03817	−0.01546	−0.00458	−0.00152
	0.9	−3.33612	2.28204	−5.61816	−5.71042	0.09217	0.00030	−0.00017	−0.00004
1.3	0.01	−7.84117	−7.77641	−0.06476	−0.05822	−0.00645	−0.00009	0.00000	0.00000
	0.1	−5.21485	−4.57237	−0.64248	−0.59645	−0.04002	−0.00539	−0.00056	−0.00007
	0.5	−4.31472	−1.12283	−3.19189	−3.21474	0.03535	−0.00969	−0.00224	−0.00058
	0.9	−3.17158	2.25890	−5.43048	−5.51334	0.08281	0.00017	−0.00010	−0.00002
		Pressure $\frac{P\sigma_0^3}{\varepsilon_0}$							
		P	P_{hs}^{BC}	$\mathbf{P_t}$	$\mathbf{P_{t1}}$	$\mathbf{P_{t2}}$	$\mathbf{P_{t3}}$	$\mathbf{P_{t4}}$	$\mathbf{P_{t5}}$
		Eq. (12)	Eq. (14)	Eq. (15)	**Series terms** Eqs. (15) and (17)				
0.7	0.01	0.00662	0.00712	−0.00050	−0.00059	−0.00012	−0.00001	0.00000	0.00000
	0.1	0.03607	0.08356	−0.04749	−0.06167	−0.00326	−0.00263	−0.00079	−0.00025
	0.5	−0.06358	0.97405	−1.03763	−1.70370	0.12320	0.02894	0.01221	0.00653
	0.9	2.86394	5.24340	−2.37945	−3.94745	−0.02134	0.01388	0.00398	0.00115
1.0	0.01	0.00950	0.01017	−0.00067	−0.00059	−0.00008	0.00000	0.00000	0.00000
	0.1	0.05408	0.11913	−0.06505	−0.06125	−0.00215	−0.00131	−0.00027	−0.00006
	0.5	−0.18195	1.36308	−1.54503	−1.65643	0.09088	0.01459	0.00431	0.00163
	0.9	3.49178	6.93010	−3.43832	−3.43718	−0.01204	0.00867	0.00183	0.00039
1.3	0.01	0.01238	0.01322	−0.00084	−0.00058	−0.00006	0.00000	0.00000	0.00000
	0.1	0.07204	0.15456	−0.08252	−0.06076	−0.00155	−0.00079	−0.00013	−0.00002
	0.5	−0.26341	1.74107	−2.00448	−1.61036	0.07324	0.00883	0.00200	0.00059
	0.9	4.04474	8.50781	−4.46307	−2.99712	−0.00704	0.00611	0.00103	0.00018

[33] was employed. For the HS formalism, Gonzalez and Silbert considered two routes, the virial (Vir) route and the mixed virial-compressibility route (CS) reported by Carnahan and Starling [34]. It is obvious from Table 2 that the free energy calculated via the present EOS compares well with computer simulation results, especially at higher temperature range in comparison with Gonzalez and Silbert results [24]. While Table 3 shows that the virial routed EOS gives closer compressibility factor to the computer simulation results than the present EOS, especially at $T^* = 1.0$, for higher temperatures, $T^* \geq 1.35$, the two results are quite close, with average deviation $\approx \pm 8\,\%$, which is not dramatic. The origin of these discrepancies could be attributed to the attractive tail contribution to the total pressure, P_t. Gonzalez and Silbert employed the Laplace transform of $g_{\mathrm{HS}}(r)$ within the PY approximation while we employed the recent approach, SMSA discussed in Section 2.

Table 2. The Helmholtz free energy of LJ fluid compared with computer simulation and other equations of states.

		F/Nk_BT			
			Theoretical calculations		
T^*	ρ^*	Present work GB–BC-SMSA	GB-Vir-PY [24]	GB–CS–PY [24]	Computer simulation MC [32]
0.75	0.6	−4.109	−4.05	−4.00	−4.24
	0.7	−4.328	−4.38	−4.22	−4.53
	0.8	−4.419	−4.52	−4.27	−4.69
1.15	0.6	−2.257	−2.12	−2.08	−2.29
	0.7	−2.181	−2.08	−1.98	−2.25
	0.8	− 1.989	− 1.92	− 1.73	− 2.06
	0.9	− 1.616	−1.59	−1.27	−1.79
1.35	0.6	−1.752	−1.62	−1.57	−1.77
	0.7	−1.596	−1.48	−1.38	−1.65
	0.8	−1.331	−1.23	−1.06	−1.41
	0.9	−0.900	−0.83	−0.55	−1.02
	0.95	−0.600	−0.56	−0.21	−0.72
2.74	0.6	−0.332	−0.21	−0.17	−0.34
	0.7	0.034	0.16	0.22	0.01
	0.8	0.478	0.59	0.70	0.43
	0.9	1.035	1.12	1.29	0.93
	1.0	1.746	1.78	2.04	1.59

Notes: GB (Gibbs–Bogoliubove variational method), BC (Baus–Colot EOS for HS reference system), Vir (Virial EOS for HS), CS (Carnahan–Starling EOS for HS), PY (Percus–Yevick approximation for $g_{HS}(r)$ for the perturbation contributions F_t and P_t), SMSA (series mean spherical approximation) and MC (Monte Carlo simulation).

Also, one of the reasons could be the numerical derivative error imposed by Gonzalez and Silbert, as in the present EOS all derivatives are performed analytically.

Next, we turn to the calculation of the VLE bimodal line, following the thermodynamic conditions for the phase equilibrium, which imply that the coexisting phases should have an equal pressure and equal chemical potential, namely

$$P(T, \rho_V) = P(T, \rho_L), \tag{19}$$

$$\mu(T, \rho_V) = \mu(T, \rho_L). \tag{20}$$

By enforcing equality of pressures and chemical potentials in the two phases at a fixed temperature, we are able to uniquely determine the densities ρ_V and ρ_L of the coexisting vapour and liquid phases. Figure 2 shows the high-temperature phase diagram of LJ fluid determined from the present EOS based on the VSMSA formalism and the NPT-MD simulation results [16]. We carried out three sets of calculations for the VLE curve for three different criteria of the effective HS diameter σ: (i) the GB method given by Equation (18); (ii) the Barker–Henderson (BH) perturbation theory [3], which leads to the explicit form

$$\sigma_{BH} = \sigma_0 \int_0^1 \left[1 - e^{-\beta\varphi_{DY}(r^*)}\right] dr^*; \tag{21}$$

Table 3. The compressibility factor for LJ fluid compared with computer simulation and other equations of states.

		$P/\rho k_B T$			
			Theoretical calculations		
T^*	ρ^*	Present work GB–BC-SMSA	GB-Vir-PY [24]	GB–CS–PY [24]	Computer simulation MC [32]
1.00	0.60	2.218	1.55	3.46	−1.60
	0.65	−0.056	−0.30	0.08	−0.25
	0.75	0.843	0.54	1.25	0.56
	0.85	2.589	2.20	3.38	2.27
	0.90	3.900	3.43	4.91	−3.5
1.35	0.10	0.718	0.78	0.78	0.72
	0.20	0.498	0.56	0.56	0.50
	0.30	0.348	0.38	0.39	0.35
	0.40	0.289	0.28	0.32	0.27
	0.50	0.375	0.34	0.44	0.30
	0.55	0.500	0.45	0.60	0.41
	0.65	0.998	0.91	1.22	0.80
	0.75	1.969	1.82	2.38	1.77
	0.85	3.641	3.36	4.29	3.37
	0.95	6.313	5.78	7.22	6.32
2.74	0.65	2.367	2.37	2.56	2.22
	0.75	3.319	3.24	3.57	3.05
	0.85	4.721	4.49	5.03	4.38
	0.95	6.725	6.22	7.04	6.15

Note: All symbols are as in Table 2.

and (iii) the Verlet and Weis (VW) [35] fitted expression,

$$\sigma_{VW} = \frac{0.3837 + 1.068/T^*}{0.4293 + 1.0/T^*}. \tag{22}$$

In this comparison we mention two important points. However, the results for the GB and BH methods are good in the vapour side but are slightly less accurate in the liquid side of the VLE curve. The curve with the GB method converges for a better critical temperature than that with the BH method. Moreover, we calculated the chemical potential μ from Equation (13), internal energy, $U = F - T(\partial F/\partial T)_\rho$, and isothermal compressibility, $\chi_T = 1/\rho(\partial\rho/\partial P)_T$ within the present EOS with the GB method. All calculations are carried out along both the vapour and liquid sides of the VLE curve of LJ fluid. The results are presented in Table 4, and compared with the NPT-MD simulations of Lotfi *et al.* [16]. It is worth mentioning that the pressure is in excellent agreement with NPT-MD results and shows the right behaviour, as it increases by increasing temperature exactly as is expected in all expanded liquids. The isothermal compressibility diverges rapidly by approaching the critical temperature, which is the typical criteria for the critical phenomena. Both the chemical potential and internal energy agree quite well with the

Table 4. Thermodynamic properties of LJ fluid along the vapour and liquid branches of the VLE curve.

			Density		Isothermal compressibility		Internal energy		Chemical potential	
	T^*	P^*	ρ^*		$\chi_T{}^*$		$-U^*$		$-\mu^*$	
			(P)	(CS)	(P)	(CS)	(P)	(CS)	(P)	(CS)
Vapour phase	1.10	0.05	0.06079	0.06179 (16)	29.33662	23.2 (24)	0.40691	0.5422 (15)	3.31189	3.3252 (14)
	1.15	0.06	0.07197	0.07366 (44)	25.75736	30.7 (22)	0.47853	0.6400 (11)	3.19092	3.1989 (24)
	1.20	0.08	0.10397	0.10715 (45)	24.97098	25.5 (15)	0.68592	0.9002 (64)	2.99998	3.0085 (10)
	1.25	0.10	0.14385	0.14630 (18)	30.25530	31.8 (42)	0.94246	1.1840 (19)	2.86126	2.8712 (24)
	1.30	0.12	0.20235	0.19290 (21)	72.83093	24.2 (89)	1.31815	1.5090	2.75174	2.7531 (15)
Liquid phase	0.70	0.00	0.82393	0.824257 (18)	0.10215	0.0847 (55)	5.55219	6.0957 (17)	5.93072	6.3000 (46)
	0.75	0.00	0.79910	0.821380 (38)	0.12077	0.0908 (32)	5.37508	5.9069 (33)	5.41721	5.6940 (28)
	0.80	0.00	0.77373	0.798870 (39)	0.14405	0.1125 (75)	5.19811	5.7102 (33)	4.98238	5.1910 (18)
	0.85	0.00	0.74751	0.775530 (24)	0.17428	0.1170 (11)	5.01436	5.5108 (21)	4.61165	4.7830 (16)
	0.90	0.01	0.72129	0.752020 (13)	0.21196	0.1540 (16)	4.82493	5.3123 (12)	4.28014	4.4338 (90)
	0.95	0.02	0.69430	0.728330 (26)	0.26119	0.1860 (21)	4.63456	5.1157 (21)	3.99224	4.1080 (18)
	1.00	0.03	0.66589	0.701790 (37)	0.32931	0.2810 (15)	4.43456	4.9018 (25)	3.74252	3.8226 (71)
	1.05	0.03	0.63276	0.671970 (44)	0.44510	0.3690 (39)	4.20392	4.6686 (32)	3.54052	3.6115 (96)
	1.10	0.05	0.60242	0.641400 (12)	0.58442	0.3850 (69)	3.99112	4.4331 (84)	3.33682	3.3910 (13)
	1.15	0.06	0.56508	0.605570 (64)	0.86001	0.6130 (99)	3.73333	4.1693 (34)	3.17315	3.2003 (43)
	1.20	0.08	0.52688	0.567800 (22)	1.30238	1.050 (12)	3.46752	3.8970 (14)	3.01613	3.0244 (46)
	1.25	0.10	0.48219	0.515700 (22)	2.25884	2.320 (48)	3.16128	3.5410 (14)	2.87867	2.8817 (35)
	1.30	0.12	0.48219	0.425900 (58)	2.25884	13.60 (40)	3.16128	2.9650 (36)	2.87867	2.7523 (48)

Notes: (P) refers to for present work and (CS) refers to the NPT-MD computer simulation data reported by Lotfi *et al.* [16]. The numbers in parentheses denote the statistical uncertainties in the last two digits. All quantities are in reduced units.

Table 5. Critical parameters of LJ fluid compared with the literature.

	T_c^*	ρ_c^*	P_c^*
Equation of state			
Present work			
(GB method Eq. (18))	1.342	0.278	0.135
(BH method Eq. (21))	1.350	0.2933	0.141
(VW method Eq. (22))	1.251	0.296	0.133
Tejiro *et al.* [38]	1.310	0.300	–
MSA [8]	1.340	0.293	–
PY [39]	1.340	0.340	–
OCT [6]	1.348	0.349	–
HRT [7]	1.329	0.314	–
Computer simulation			
Johnson *et al.* [17]	1.313	0.310	0.130
MC [15]	1.316	0.304	–
MC [19]	1.312	0.316	0.1279
MC [18]	1.326	0.316	–
GEMC [14]	1.3	0.317	–
MC [12]	1.3	0.33	0.130
MC [11]	1.36	0.36	–
NPT-MD [20]	1.313	0.304	0.125
NPT-MD [16]	1.310	0.314	0.126
MD [13]	1.35	0.35	0.142

Notes: GB, BH and VW stand for Gibbs–Bogoliubove, Barker–Henderson and Verlet and Weis perturbation methods, respectively. MC and MD refer to Monte Carlo and molecular dynamics simulations.

computer simulation results. They change slightly along the VLE curve, which is typically the case for fluids with long-range attractive forces, like LJ fluid.

Figure 2 highlights the main idea that all VLE curves fail to show good performance in the near vicinity of the critical point, with large uncertainty in determining the critical parameters T_C and ρ_C. This is a strong indication that the behaviour of the fluid near criticality is independent of the kind of perturbation or variational scheme used. This is an inherited problem due to the lack of knowledge on the correlation function treatment at the near vicinity of the critical point. Instead, the critical parameters T_C, ρ_C and P_C can be estimated by extrapolation analysis of the available values in the near critical region, following a fitting procedure used by several authors [36,37]; the VLE critical point was determined by assuming the scaling law $\rho_L - \rho_V = C(T_C - T)^{0.32}$ and the law of rectilinear diameters $\rho_L + \rho_V = 2\rho_C + D(T - T_C)$ where C and D are fitting parameters. The exponent 0.32 represents the critical exponent in case of classical fluids. Then the values of T_C and ρ_C can be inserted in Equation (12) to obtain the critical pressure, P_C. Our estimated values of the critical parameters of LJ fluid are presented in Table 5, collectively with the results of most of the previous calculations. For the GB method, our estimate of T_C agrees well with the molecular dynamics simulation results [13] and with the theoretical results [6,8,39], while our estimate of critical pressure, P_C, is slightly overestimated and our critical density ρ_C is relatively underestimated, compared to most of the reported calculations.

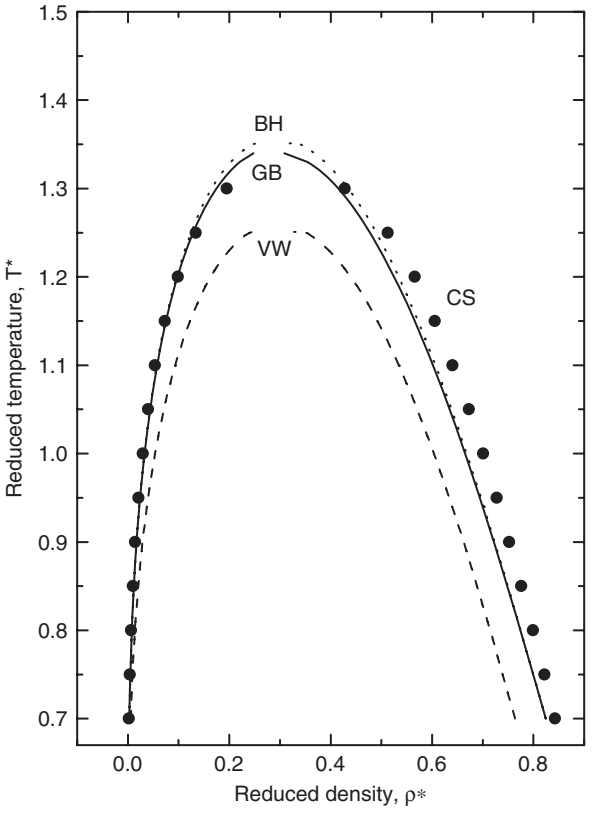

Figure 2. Liquid–vapour coexistence curve of LJ fluid obtained from the present EOS using three methods for calculating the effective HS diameter, σ: Gibbs–Bogoliubov method [9] (solid line), Barker–Henderson method [3] (dotted line) and Verlet and Weis method [35] (dashed line). Results of the molecular dynamic computer simulation of Lotfi *et al.* [16] are also shown (solid circles).

4. Conclusions

The authors show that the DY potential, with suitably chosen parameters, in conjunction with the variational theory based on BC [31] scaled HS formalism and on the SMSA [22], provides a simple analytic expression for the thermodynamic properties of simple fluids.

Moreover, the authors discuss the reasons that the combination of the BC and the SMSA, within the GB variational method, form the best EOS, which leads to a good agreement with the computer simulation results and is consistent with the earlier theoretically-based equations of state. However, the present EOS predicts pressures, internal energies, isothermal compressibilities and chemical potentials which are in relatively good agreement with computer simulations. The liquid density is slightly underestimated. The thermodynamic properties of the vapour side of the VLE curve are in excellent agreement with computer simulation results, which may be related to the nature of the high-temperature expansion formalism employed in the present work.

Quite recently, we applied the present EOS to investigate the thermodynamic properties of C_{60} [28] by fitting the DY potential to the Garifalco potential [40]. The

performance of the present EOS was remarkably good – comparable to the computer simulation and to the other theoretical models. On the other hand, Tejero *et al*. [38,41] showed the applicability of the DY potential to colloidal fluids, as well as to monatomic fluids.

Acknowledgements

We are grateful to the Sultan Qaboos University for the research project # IG/Sci/Phys/07/04 and its substantial financial support for completing this work.

References

[1] W.H. Young, Rep. Prog. Phys. **55**, 1769 (1992).
[2] J.P. Hansen and I.R. McDonald, *Theory of Simple Liquids*, 1st ed. (Academic Press, London, 1976).
[3] J.A. Barker and D. Henderson, Rev. Mod. Phys. **47**, 587 (1976).
[4] J.D. Weeks, D. Chandler, and H.C. Andersen, J. Chem. Phys. **54**, 5237 and **55**, 5422 (1971).
[5] D. Henderson and J.A. Barker, Rev. Mod. Phys. **48**, 587 (1976).
[6] S.H. Sung and D. Chandler, Phys. Rev. A **9**, 1688 (1974).
[7] M. Tau, A. Parola, D. Pini, and L. Reatto, Phys. Rev. E **52**, 2644 (1995).
[8] Yu.V. Kalyuzhnyi and P.T. Cummings, Molec. Phys. **87**, 1459 (1996).
[9] H. Jones, J. Chem. Phys. **55**, 2640 (1971).
[10] S.M. Osman and W.H. Young, Phys. Chem. Liq. **17**, 181 (1987).
[11] J.P. Hansen and L. Verlet, Phys. Rev. **184**, 151 (1969).
[12] D.J. Adams, Molec. Phys. **37**, 211 (1976); **32**, 647 (1976).
[13] J.J. Nicolas, K.E. Gubbins, W.B. Streett, and D.J. Tildesley, Molec. Phys. **37**, 1429 (1979).
[14] E.N. Rudisill and P.T. Cummings, Molec. Phys. **68**, 629 (1989).
[15] B. Smit, J. Chem. Phys. **96**, 8639 (1992).
[16] A. Lotfi, J. Vrabec, and J. Fischer, Molec. Phys. **76**, 1319 (1992).
[17] J.K. Johnson, J.A. Zollweg, and K.E. Gubbins, Molec. Phys. **78**, 591 (1993).
[18] J.M. Caillol, J. Chem. Phys. **109**, 4885 (1998).
[19] J.J. Potoff and A.Z. Panagiotopoulos, J. Chem. Phys. **109**, 10914 (1998).
[20] H. Okumura and F. Yonezawa, J. Chem. Phys. **113**, 9162 (2000).
[21] D. Henderson, L. Blum, and J.P. Noworyta, J. Chem. Phys. **102**, 4973 (1995).
[22] D.-M. Duh and L. Mier-y-Teran, Mol. Phys. **90**, 373 (1997).
[23] S.M. Foiles and N.W. Ashcroft, J. Chem. Phys. **75**, 3594 (1981).
[24] D. Gonzalez and M. Silbert, J. Phys. C; Solid State Phys. **16**, L1097 (1983).
[25] R. Garcia and D. Gonzalez, Phys. Chem. Liq. **18**, 91 (1988).
[26] S.M. Osman and I. Ali, Int. J. Mod. Phys. B **13**, 1419 (1999).
[27] I. Ali, S.M. Osman, M.S. Al-Busaidi, and R.N. Singh, Int. J. Modern Phys. B **13**, 3261 (1999).
[28] M.B. Khedr, M.S. Al-Busaidy, and S.M. Osman, J. Phys. Cond. Matter **17**, 4411 (2005).
[29] A.Z. Panagiotoulos, Molec. Phys. **100**, 237 (2002).
[30] P.T. Commings and E.R. Smith, Chem. Phys. **42**, 241 (1979) and Molec. Phys. **38**, 997 (1979).
[31] M. Baus and J.L. Colot, Phys. Rev. A **36**, 3912 (1987).
[32] J.P. Hansen, Phys. Rev. A **2**, 221 (1970).
[33] M.S. Wertheim, Phys. Rev. Lett. **10**, 321 (1963).
[34] N.F. Carnahan and K.E. Starling, J. Chem. Phys. **51**, 635 (1969).
[35] L. Verlet and J.J. Weis, Phys. Rev. A **5**, 939 (1972).
[36] C. Caccamo, D. Costa, and A. Fucile, J. Chem. Phys. **106**, 225 (1997).
[37] J.A. Alonso, M.J. Lopez, N.H. March, and D. Lamoen, Phys. Chem. Liq. **40**, 457 (2002).

[38] C.F. Tejero, A. Daanoun, H.N.W. Lekkerkerker, and M. Baus, Phys. Rev. Lett. **73**, 752 (1994).
[39] D.J. Henderson, J.A. Barker, and R.O. Watts, IBM J. Res. Dev. **14**, 68 (1970).
[40] L.A. Garifalco, J. Phys. Chem. **96**, 858 (1992).
[41] C.F. Tejero, A. Daanoun, H.N.W. Lekkerkerker, and M. Baus, Phys. Rev. E **51**, 558 (1995).